Supplementary Information

Facet-dependent synthesis of H_2O_2 from H_2 and O_2 over single-atom Pt modified Pd nanocrystal catalysts

Ying Zhang,[a] Qingdi Sun,[a] Ziyue Wang,[a] Guanghui Guo,[a] Hao Liu,[a] Xiaohui He*[ac] and Hongbing Ji*[ab]

[a] Key Laboratory of Bioinorganicand Synthetic Chemistry of Ministry of Education, Fine Chemical Industry Research Institute, School of Chemistry, IGCME, Sun Yat-sen University, Guangzhou 510275, China.

[b] State Key Laboratory Breeding Base of Green-Chemical Synthesis Technology, Institute of Green Petroleum Processing and Light Hydrocarbon Conversion, College of Chemical Engineering, Zhejiang University of Technology, Hangzhou, 310014 P. R. China.

[c] Guangdong Technology Research Center for Synthesis and Separation of Thermosensitive Chemicals.

*Corresponding Author(s): Hongbing Ji: jihb@mail.sysu.edu.cn; Xiaohui He: hexiaohui@mail.sysu.edu.cn.

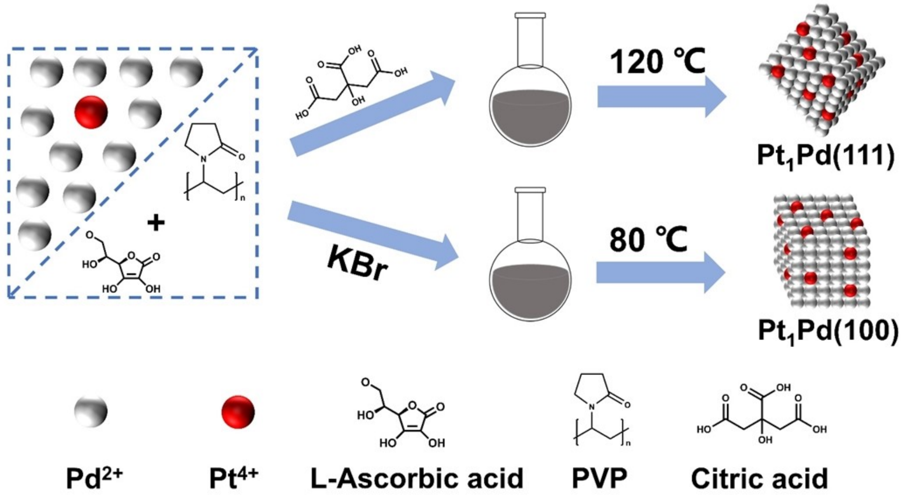

Figure S1. Schematic illustration of the synthetic pathways leading to the formation of the $Pt_1Pd(111)$ and $Pt_1Pd(100)$ nanocrystal.

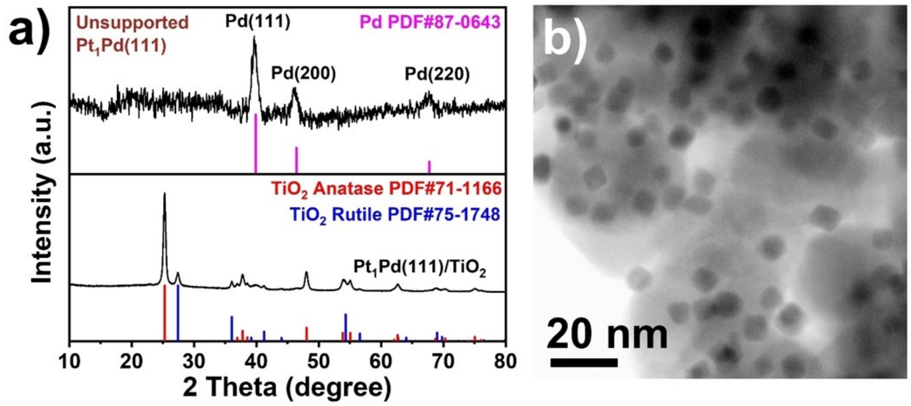

Figure S2. a) PXRD patterns of $Pt_1Pd(111)$ nanocrystal and $Pt_1Pd(111)/TiO_2$. b) Bright-fields STEM image of $Pt_1Pd(111)/TiO_2$.

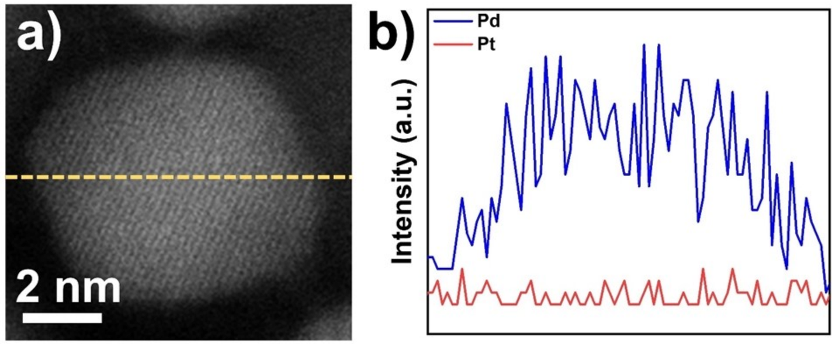

Figure S3. a) HAADF-STEM image of $Pt_1Pd(111)$ nanocrystal on TiO_2. b) Elemental line-scan profiles along the direction marked by a yellow line in a).

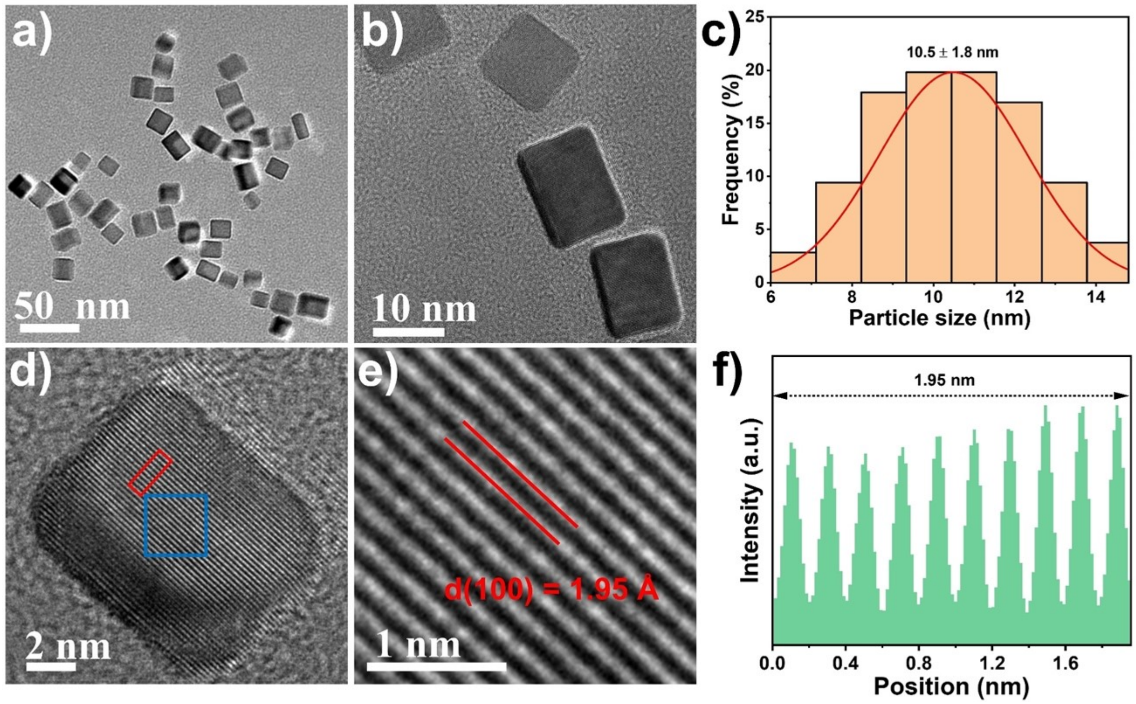

Figure S4. Morphology and structure representation of monodispersed $Pt_1Pd(100)$ nanocrystal. a) Representative TEM image. b, d) High-resolution TEM images. c) Particle size distribution of $Pt_1Pd(100)$ nanocrystal. e) Magnified TEM image in the blue box from d). f) Intensity profile of the red box from d).

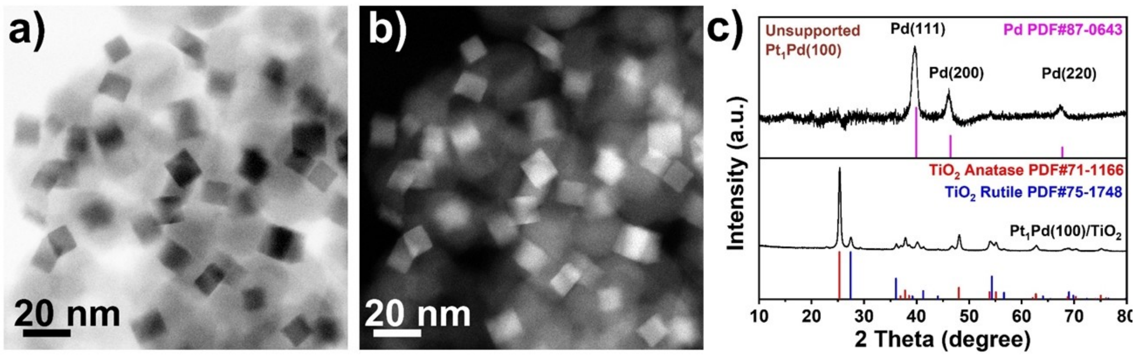

Figure S5. a) Bright-fields and b) dark-fields STEM images of $Pt_1Pd(100)/TiO_2$. c) PXRD patterns of $Pt_1Pd(100)$ nanocrystal and $Pt_1Pd(100)/TiO_2$.

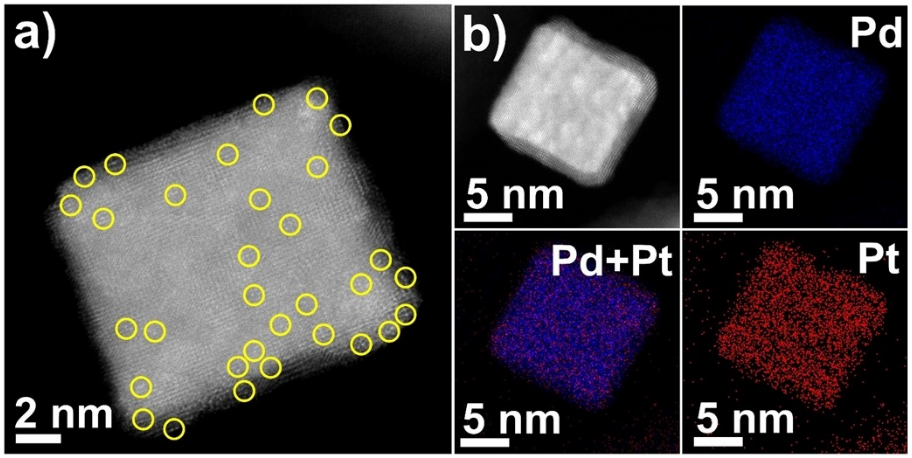

Figure S6. a) AC HAADF-STEM image of $Pt_1Pd(100)/TiO_2$, Pt single atoms are highlighted by the yellow circles. b) EDS mapping of $Pt_1Pd(100)/TiO_2$.

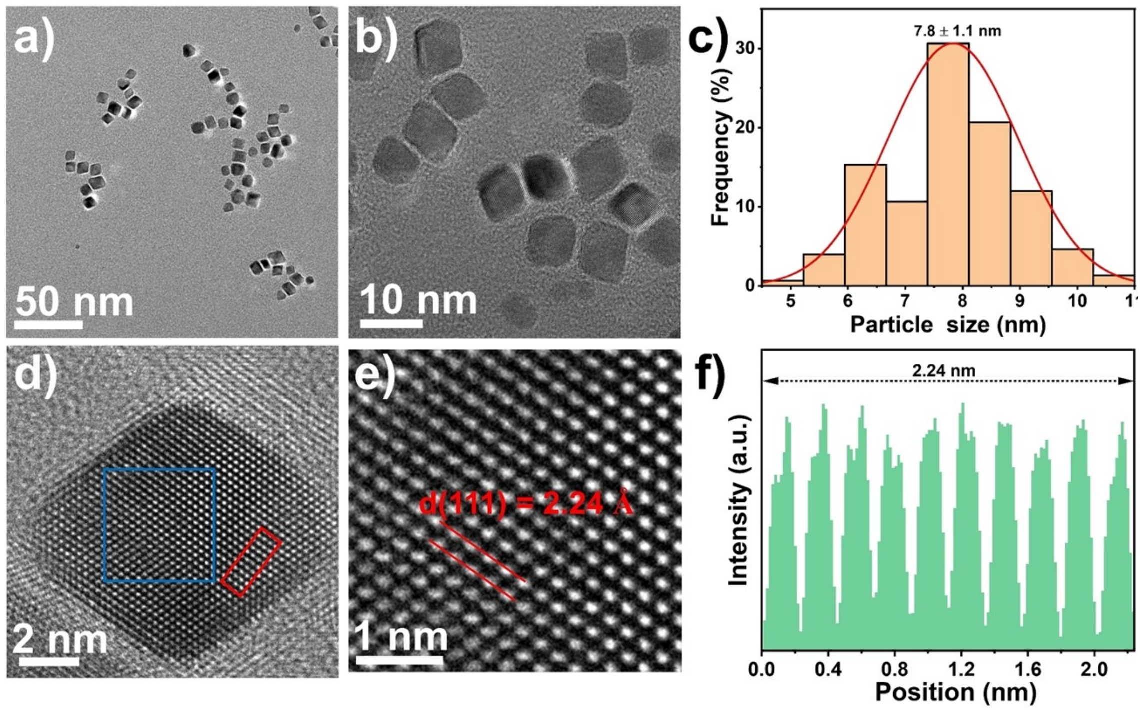

Figure S7. Morphology and structure representation of monodispersed Pd(111) nanocrystal. a) Representative TEM image. b, d) High-resolution TEM images. c) Particle size distribution of Pd(111) nanocrystal. e) Magnified TEM image in the blue box from d). f) Intensity profile of the red box from d).

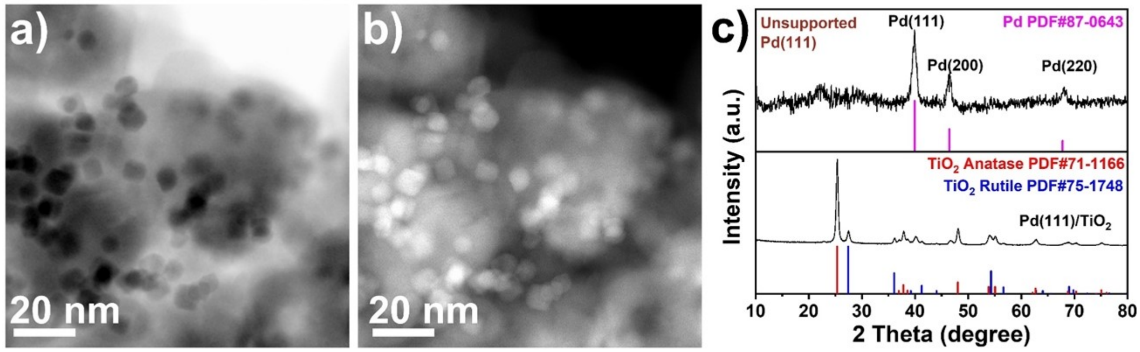

Figure S8. a) Bright-fields and b) dark-fields STEM images of Pd(111)/TiO_2. c) PXRD patterns of Pd(111) nanocrystal and Pd(111)/TiO_2.

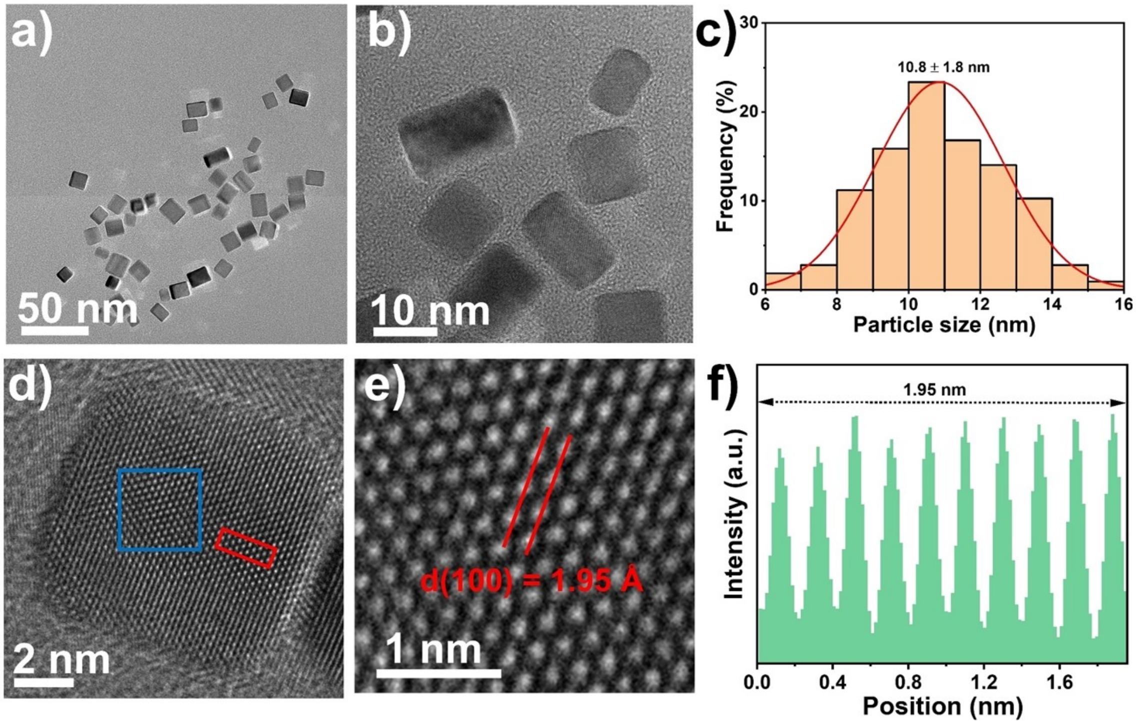

Figure S9. Morphology and structure representation of monodispersed Pd(100) nanocrystal. a) Representative TEM image. b, d) High-resolution TEM images. c) Particle size distribution of Pd(100) nanocrystal. e) Magnified TEM image in the blue box from d). f) Intensity profile of the red box from d).

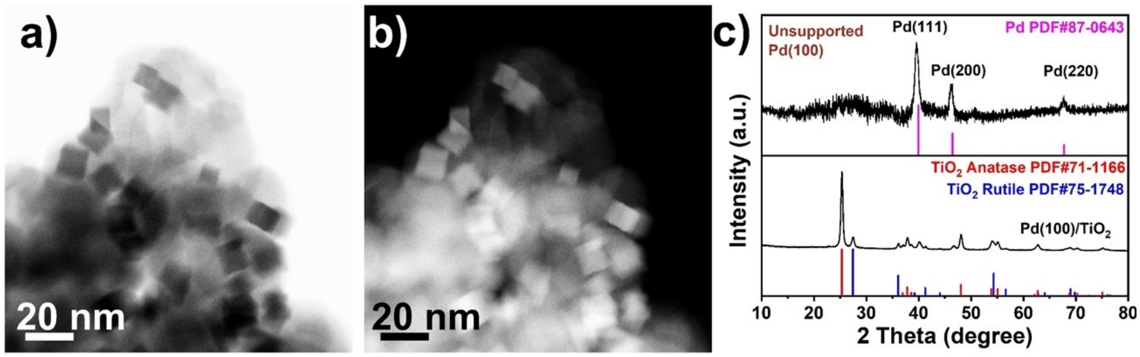

Figure S10. a) Bright-fields and b) dark-fields STEM images of Pd(100)/TiO_2. c) PXRD patterns of Pd(100) nanocrystal and Pd(100)/TiO_2.

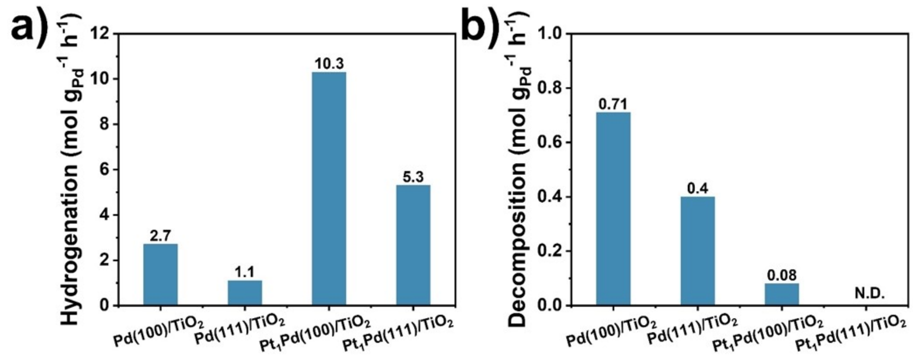

Figure S11. Comparison of H_2O_2 a) hydrogenation and b) decomposition on various catalysts. Reaction condition: a) 10 mL CH_3OH, H_2O_2: 250 µL, 0.02 M HCl, 2.9 MPa 5% H_2/N_2, T = 0 °C, catalyst weight: 10 mg, and stirring: 1200 rpm. b) 10 mL CH_3OH, H_2O_2: 250 µL, 0.02 M HCl, 4 MPa N_2, T = 0 °C, catalyst weight: 10 mg, and stirring: 1200 rpm.

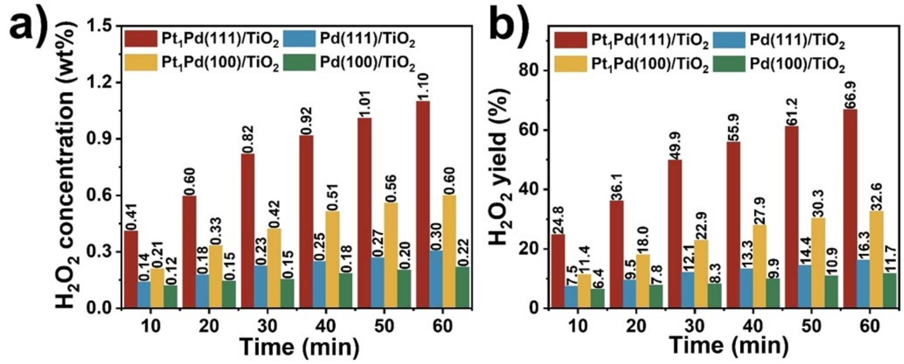

Figure S12. Comparison of a) H_2O_2 concentration and b) H_2O_2 yield as a function of reaction time towards H_2O_2 synthesis. Reaction condition: 10 mL CH_3OH, 0.02 M HCl, 2.9 MPa 5% H_2/N_2, 1.1 MPa 25% O_2/N_2, T = 0 °C, catalyst weight: 10 mg, and stirring: 1200 rpm.

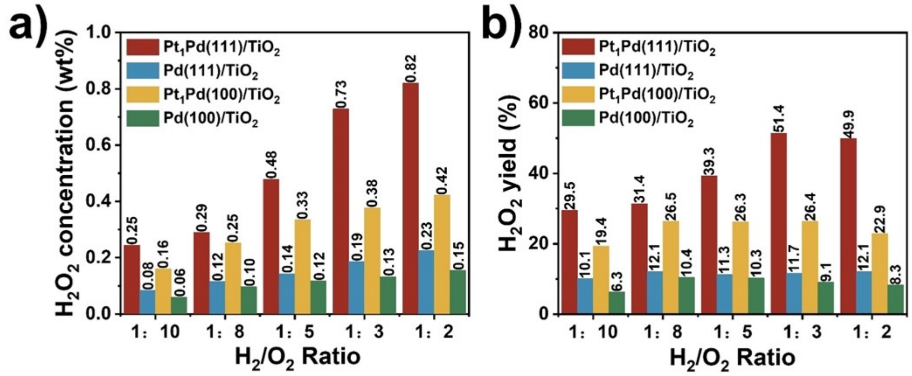

Figure S13. Comparison of a) H_2O_2 concentration and b) H_2O_2 yield with different H_2/O_2 ratio towards H_2O_2 synthesis. Reaction condition: 10 mL CH_3OH, 0.02 M HCl, T = 0 °C, catalyst weight: 10 mg, time: 30 minutes, and stirring: 1200 rpm.

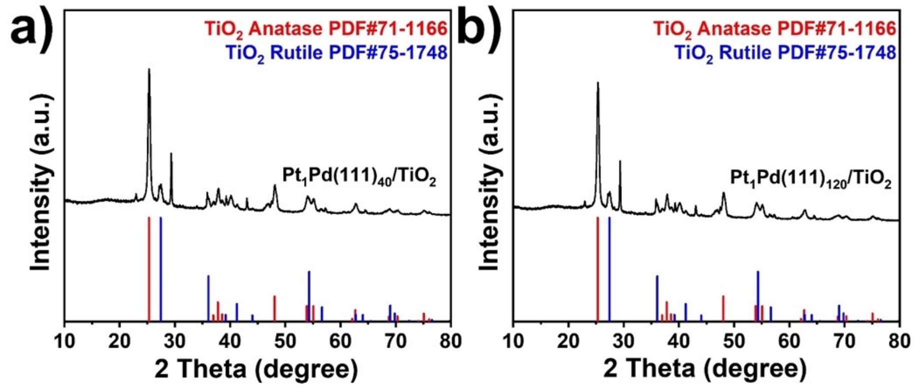

Figure S14. PXRD patterns of a) $Pt_1Pd(111)_{40}/TiO_2$ and b) $Pt_1Pd(111)_{120}/TiO_2$.

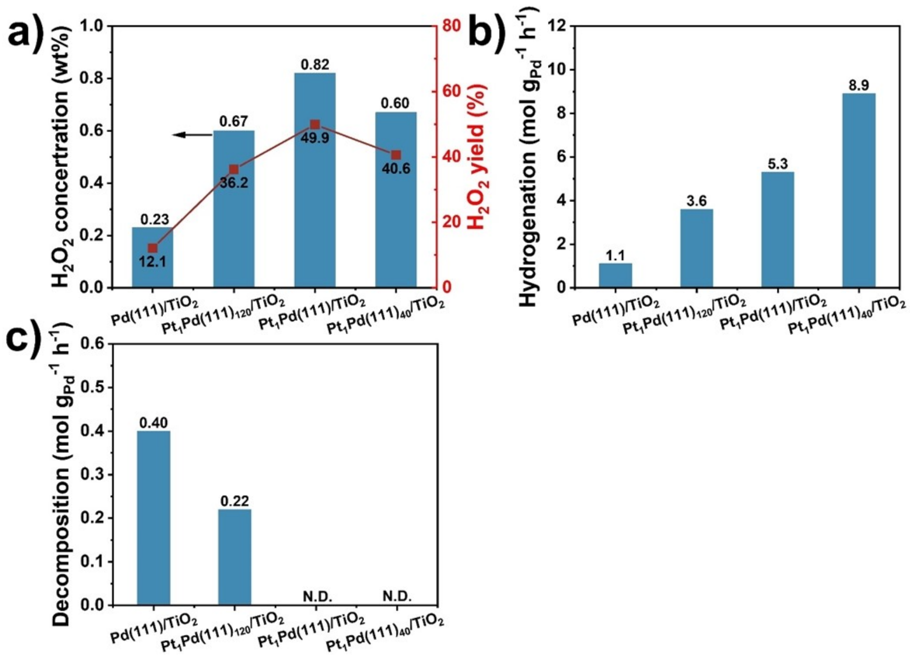

Figure S15. a) H_2O_2 concentration and H_2 yield, b) H_2O_2 hydrogenation, and c) H_2O_2 decomposition with different Pd/Pt atomic ratio in direct synthesis of H_2O_2. Reaction condition: a) 10 mL CH_3OH, 0.02 M HCl, 2.9 MPa 5% H_2/N_2, 1.1 MPa 25% O_2/N_2, T = 0 °C, catalyst weight: 10 mg, time: 30 minutes, and stirring: 1200 rpm. b) 10 mL CH_3OH, H_2O_2: 250 μL, 0.02 M HCl, 2.9 MPa 5% H_2/N_2, T = 0 °C, catalyst weight: 10 mg, and stirring: 1200 rpm. c) 10 mL CH_3OH, H_2O_2: 250 μL, 0.02 M HCl, 4 MPa N_2, T = 0 °C, catalyst weight: 10 mg, and stirring: 1200 rpm.

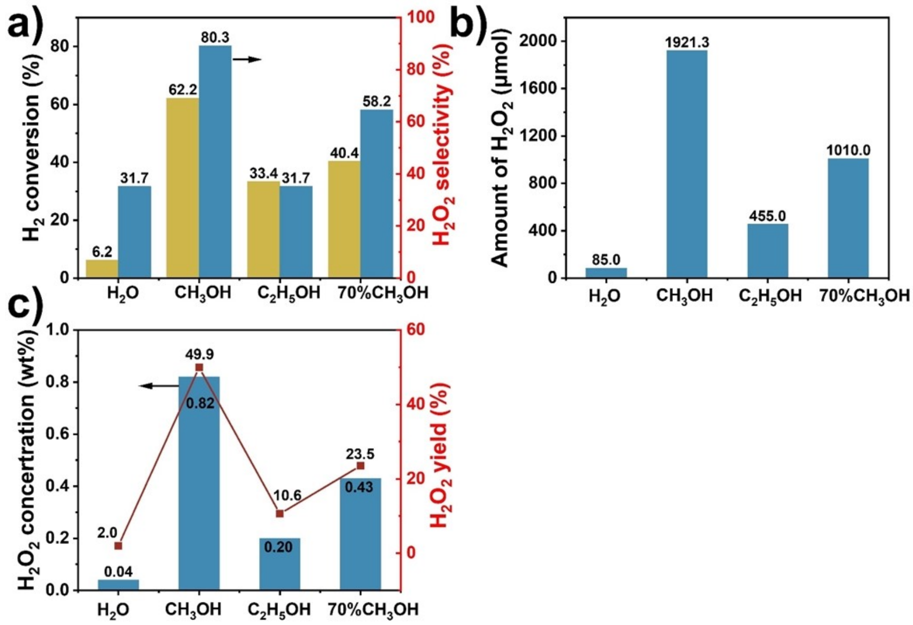

Figure S16. Comparison of a) H_2 conversion and H_2O_2 selectivity, b) amount of H_2O_2 and c) H_2O_2 concentration and H_2O_2 yield towards H_2O_2 synthesis with different solvents. Reaction condition: 10 mL solvent, 0.02 M HCl, 2.9 MPa 5% H_2/N_2, 1.1 MPa 25% O_2/N_2, T = 0 °C, catalyst weight: 10 mg, time: 30 minutes, and stirring: 1200 rpm.

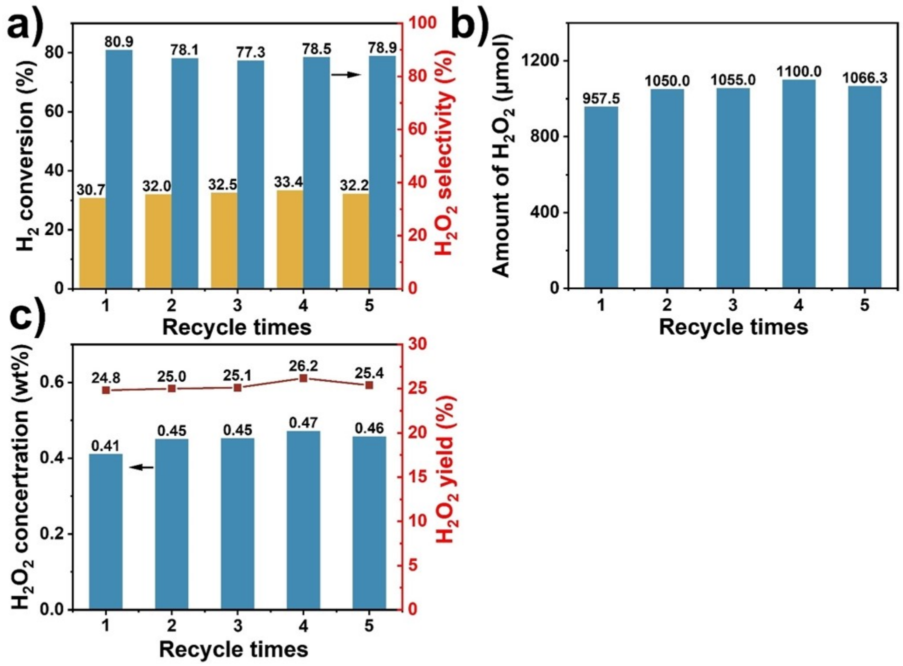

Figure S17. Stability test on $Pt_1Pd(111)/TiO_2$ in 5 cycles. a) H_2 conversion and H_2O_2 selectivity, b) amount of H_2O_2, and c) H_2O_2 concentration and H_2O_2 yield in 5 cycles. Reaction condition: 10 mL CH_3OH, 0.02 M HCl, 2.9 MPa 5% H_2/N_2, 1.1 MPa 25% O_2/N_2, T = 0 °C, catalyst weight: 10 mg, time: 10 minutes, and stirring: 1200 rpm.

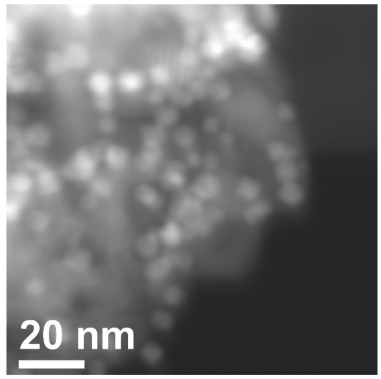

Figure S18. STEM image of $Pt_1Pd(111)/TiO_2$ after reaction.

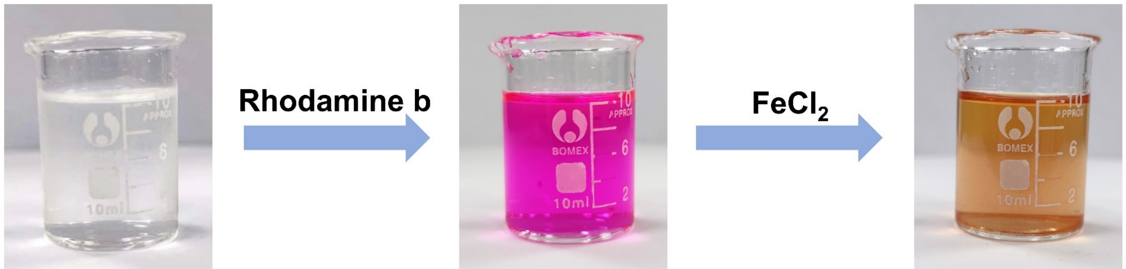

Figure S19. The photographs of a) as-synthesized H_2O_2 solution, (b) rhodamine b (20 ppm) in the as-synthesized H_2O_2 solution, and (c) the liquor after Fenton reaction using $FeCl_2$.

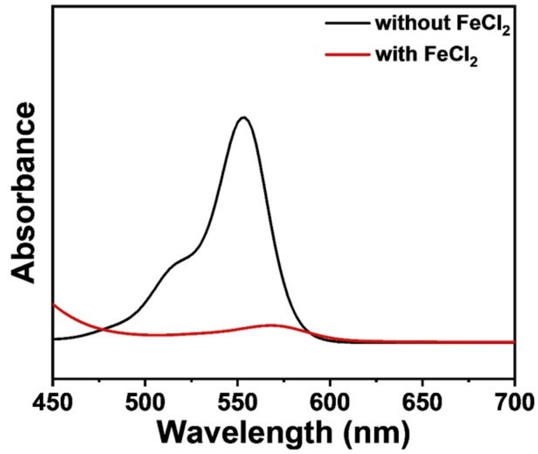

Figure S20. UV-Vis spectra of rhodamine b (20 ppm) in the as-synthesized H_2O_2 solution and the liquor after Fenton reaction using $FeCl_2$.

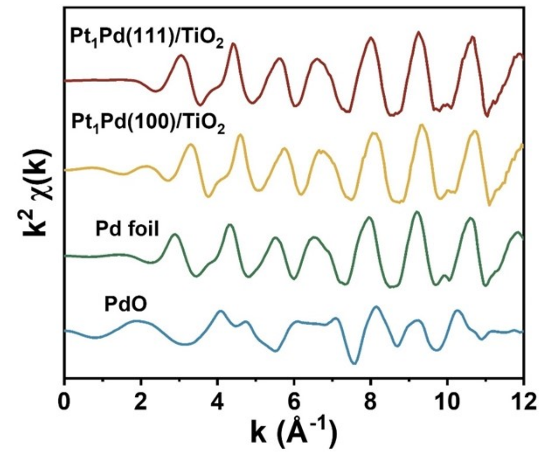

Figure S21. Pd K-edge XANES profiles in K space.

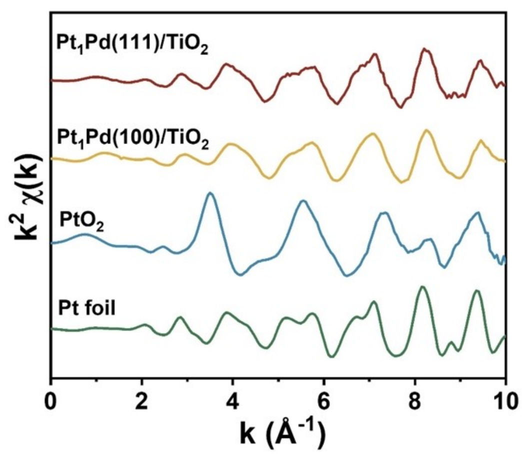

Figure S22. Pt L3-edge XANES profiles in K space.

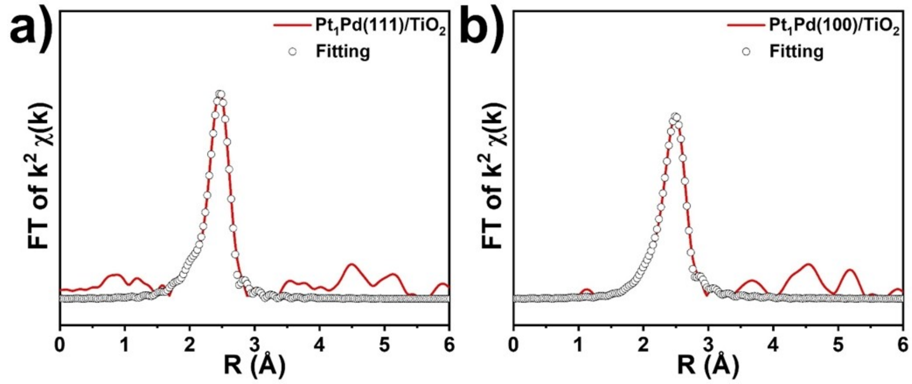

Figure S23. R-space fitting curves for the Pd K-edge of a) $Pt_1Pd(111)/TiO_2$, and b) $Pt_1Pd(100)/TiO_2$.

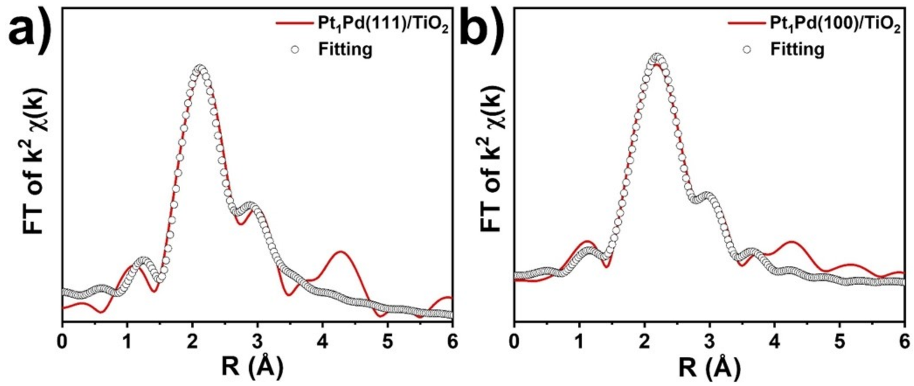

Figure S24. R-space fitting curves for the Pt L3-edge of a) $Pt_1Pd(111)/TiO_2$ and b) $Pt_1Pd(100)/TiO_2$.

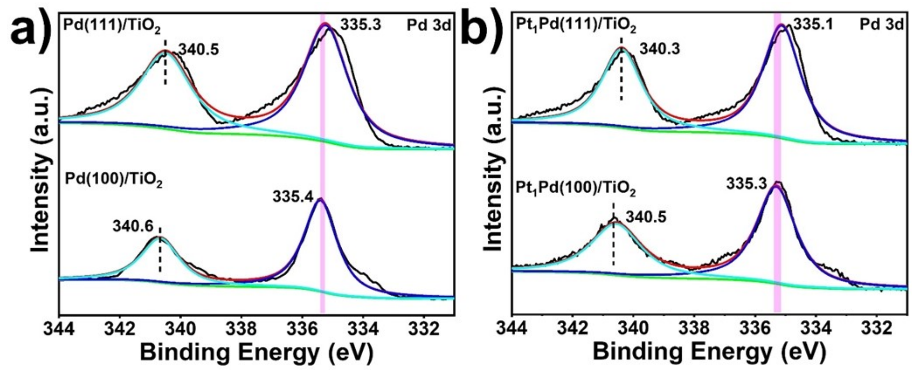

Figure S25. a) Pd 3d XPS spectra of Pd(111)/TiO_2 and Pd(100)/TiO_2. b) Pd 3d XPS spectra of Pt_1Pd(111)/TiO_2 and Pt_1Pd(100)/TiO_2.

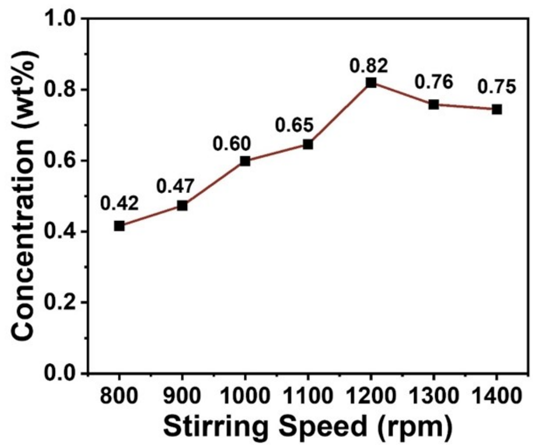

Figure S26. The comparison of H_2O_2 concentration on $Pt_1Pd(111)/TiO_2$ in the direct synthesis of H_2O_2 under different stirring rate.

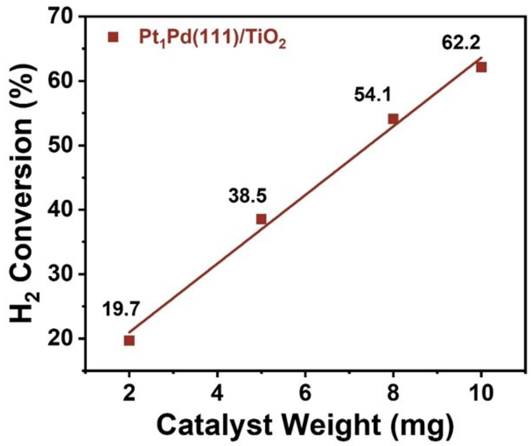

Figure S27. The comparison of H_2 conversion on $Pt_1Pd(111)/TiO_2$ in the direct synthesis of H_2O_2 with different catalyst weight.

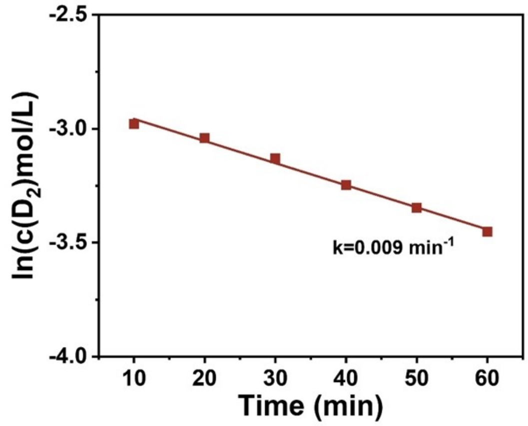

Figure S28. The apparent rate constant for D_2O_2 synthesis using D_2.

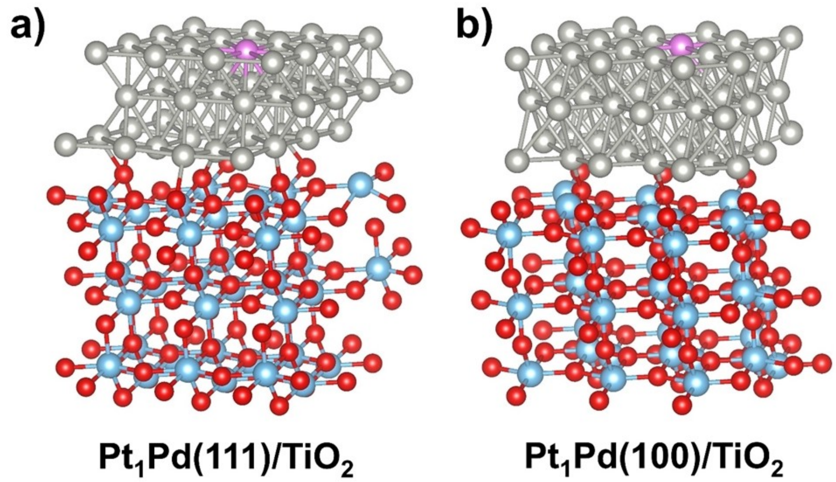

Figure S29. The structure models of $Pt_1Pd(111)/TiO_2$ and $Pt_1Pd(100)/TiO_2$. The pink, gray, red, and light blue spheres represent Pt, Pd, O, and Ti atoms, respectively.

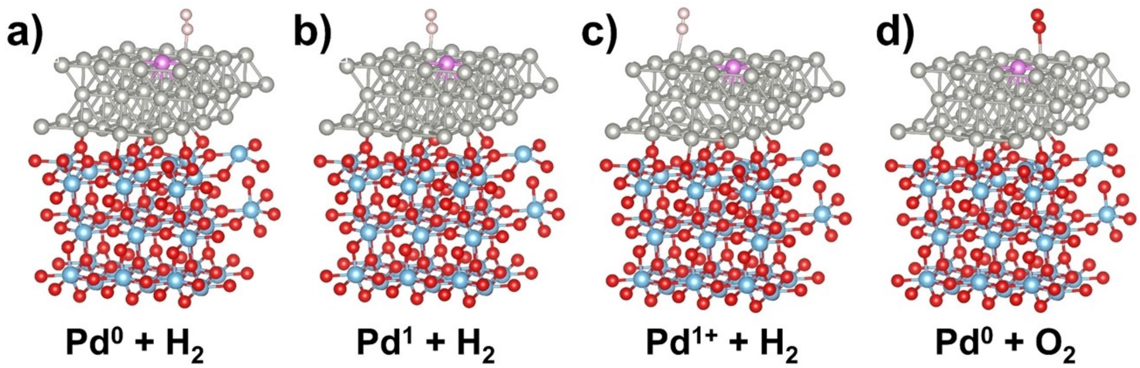

Figure S30. The adsorption structure models of H_2 on $Pt_1Pd(111)/TiO_2$. a) H_2 adsorbed at the Pd site (Pd^0) connected to Pt atom. b) H_2 adsorbed at the Pd site (Pd^1) away from Pt atom. c) H_2 adsorbed at the Pd site (Pd^{1+}) further away from Pt atom. d) O_2 adsorbed at the Pd site (Pd^0) connected to Pt atom.

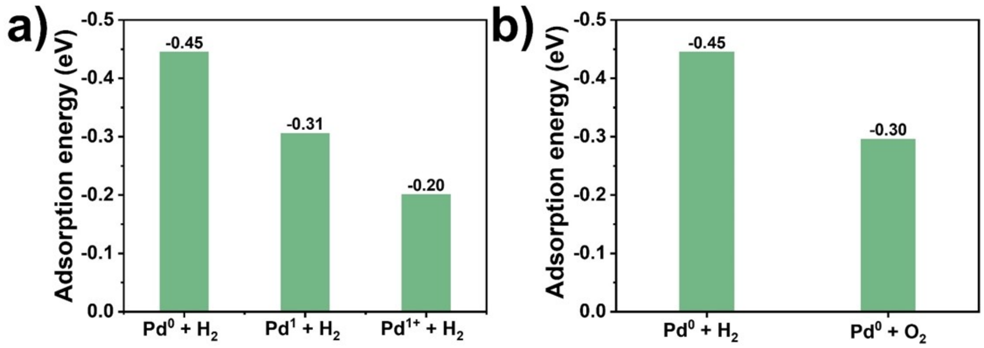

Figure S31. a) The adsorption energies of H_2 on different Pd sites over $Pt_1Pd(111)/TiO_2$. b) The adsorption energies of H_2 and O_2 on the Pd site connected to Pt atom over $Pt_1Pd(111)/TiO_2$.

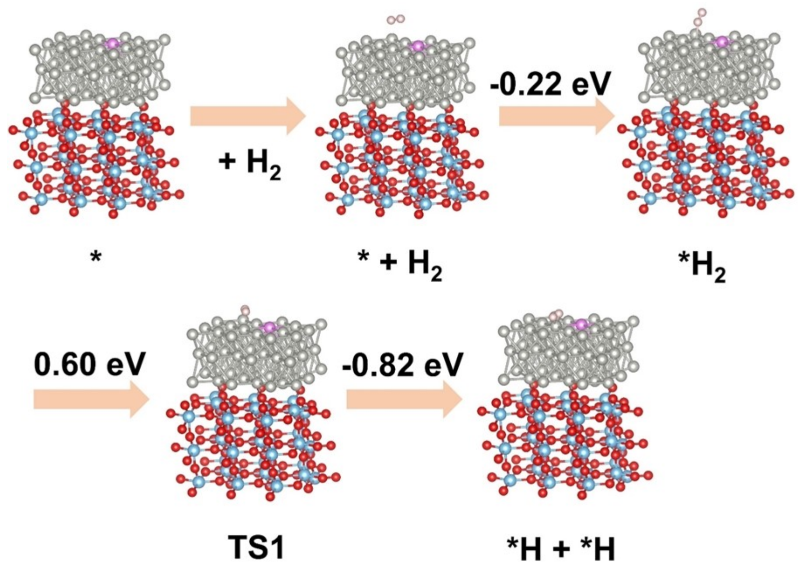

Figure S32. The process of H_2 dissociation on $Pt_1Pd(100)/TiO_2$.

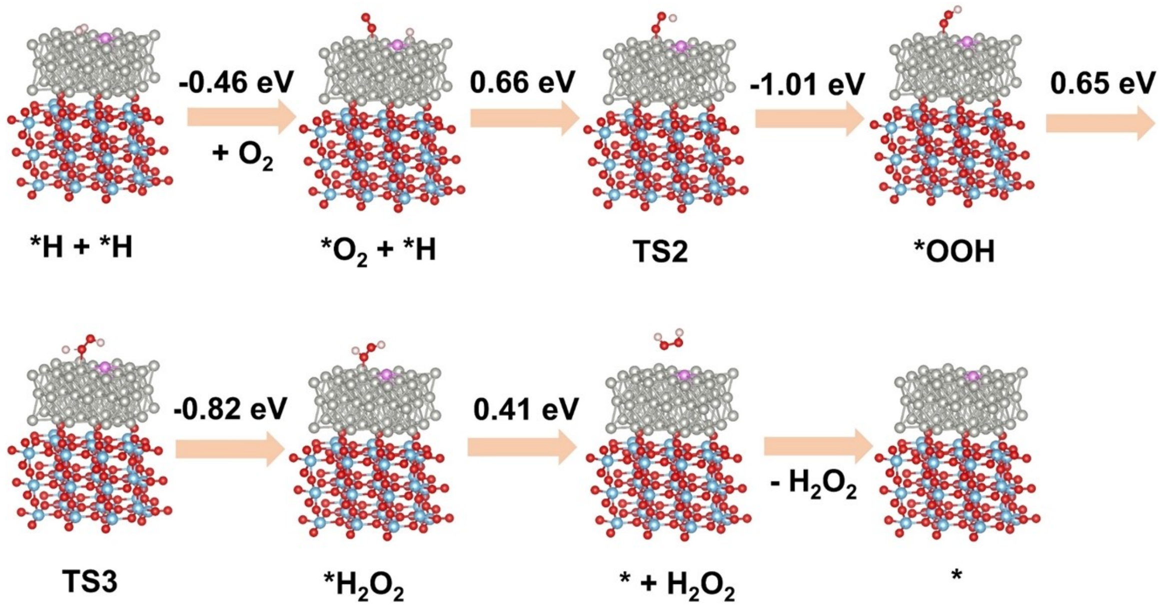

Figure S33. The process of O_2 hydrogenation to H_2O_2 on $Pt_1Pd(100)/TiO_2$.

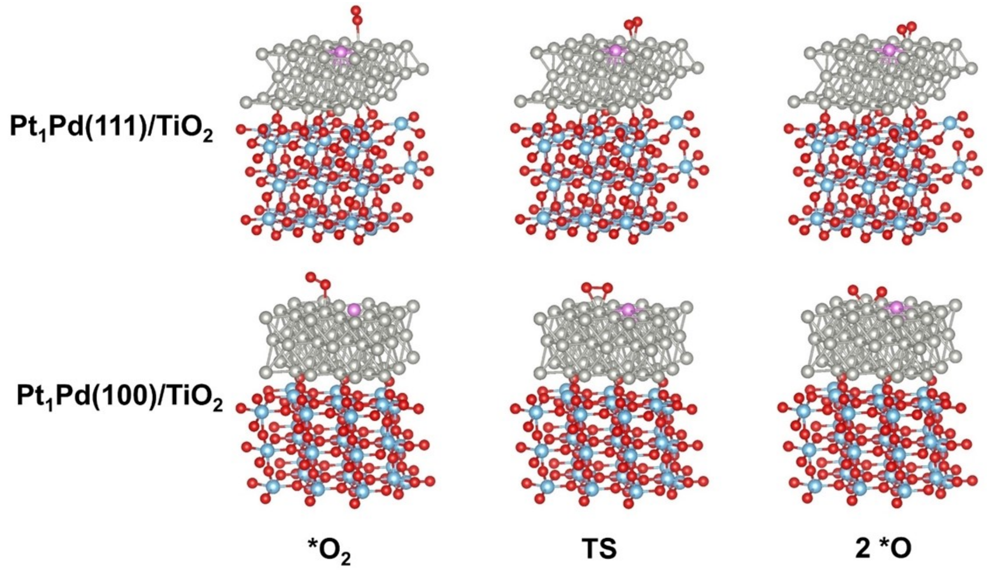

Figure S34. The process of $*O_2$ dissociation on $Pt_1Pd(111)/TiO_2$ and $Pt_1Pd(100)/TiO_2$.

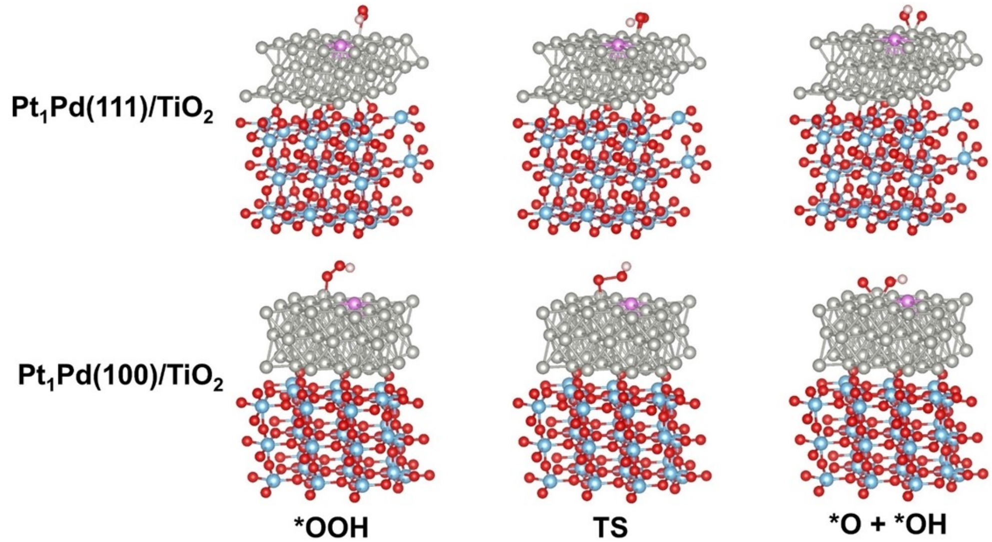

Figure S35. The process of *OOH dissociation on $Pt_1Pd(111)/TiO_2$ and $Pt_1Pd(100)/TiO_2$.

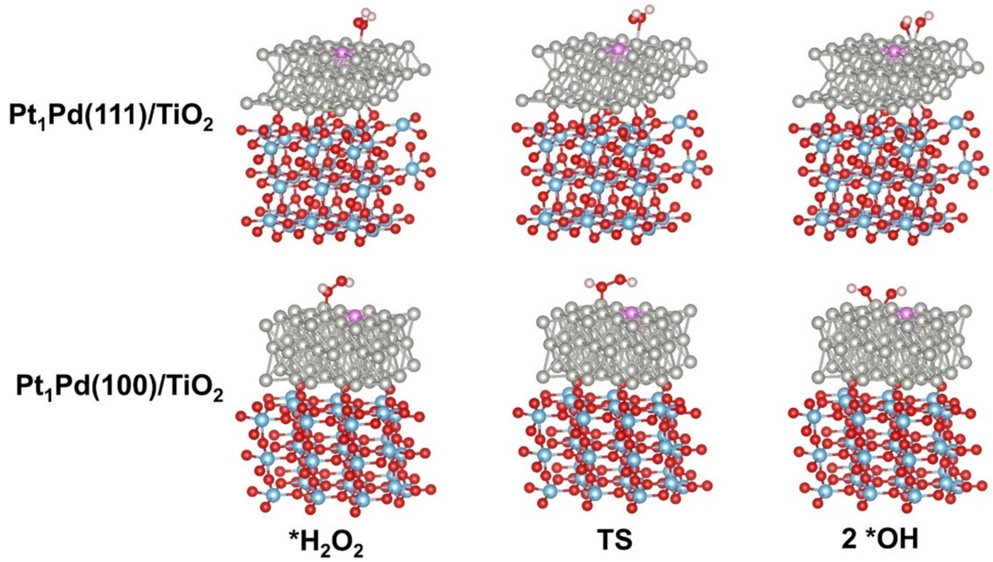

Figure S36. The process of $*H_2O_2$ dissociation on $Pt_1Pd(111)/TiO_2$ and $Pt_1Pd(100)/TiO_2$.

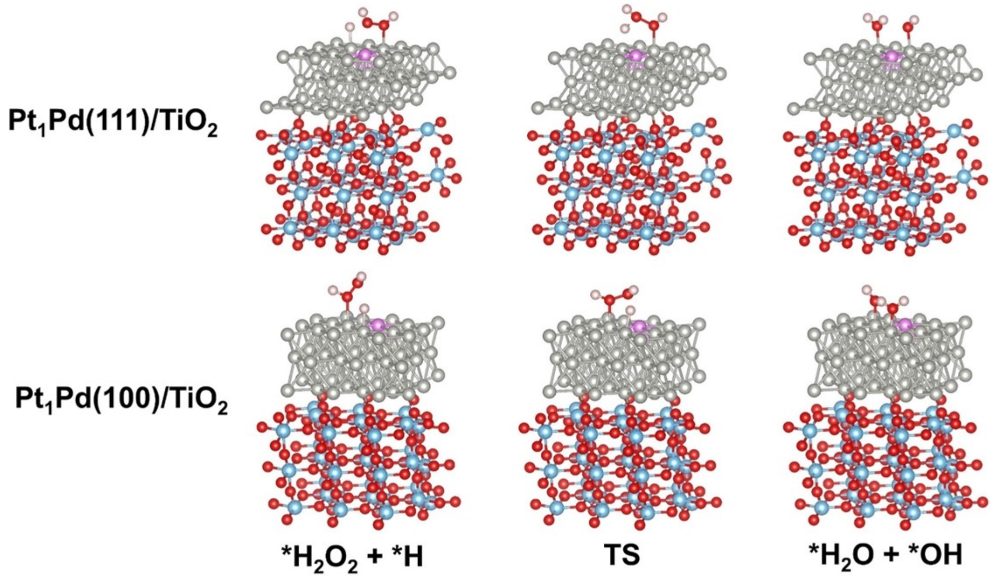

Figure S37. The process of *H_2O_2 hydrogenation on $Pt_1Pd(111)/TiO_2$ and $Pt_1Pd(100)/TiO_2$.

Table S1. Elemental analysis of various catalysts.

Entry	Catalysts	Pd/Pt (atomic ratio)	Nominal loading		Actual loading[a]	
			Pd (wt%)	Pt (wt%)	Pd (wt%)	Pt (wt%)
1	$Pt_1Pd(111)/TiO_2$	80	3.5	0.075	3.3	0.09
2	$Pt_1Pd(100)/TiO_2$	80	3.5	0.075	3.4	0.08
3	$Pd(111)/TiO_2$	-	3.5	-	3.2	-
4	$Pd(100)/TiO_2$	-	3.5	-	3.6	-
5	$Pt_1Pd(111)_{40}/TiO_2$	40	3.5	0.150	3.7	0.17
6	$Pt_1Pd(111)_{120}/TiO_2$	120	3.5	0.050	3.5	0.07
7	$Pt_1Pd(111)/TiO_2$-used	80	3.5	750	3.2	0.09

[a]Determined by ICP-AES.

Table S2. EXAFS fitting parameters at the Pd K-edge for $Pt_1Pd(111)/TiO_2$ and $Pt_1Pd(100)/TiO_2$.

Sample	Shell	C. N.	R(Å)	σ^2 (Å^2)	ΔE_0 (eV)	R factor
$Pt_1Pd(111)/TiO_2$	Pd–Pd	11.6±0.8	2.74±0.005	0.053±0.001	3.0±0.5	0.011
	Pd–Pt	0.8±0.9	2.68±0.03	0.003±0.003		
$Pt_1Pd(100)/TiO_2$	Pd–Pd	11.5±0.6	2.74±0.003	0.002±0.001	3.2±0.4	0.005
	Pd–Pt	0.6±0.5	2.70±0.02	0.002±0.002		

Table S3. EXAFS fitting parameters at the Pt L_3-edge for $Pt_1Pd(111)/TiO_2$ and $Pt_1Pd(100)/TiO_2$.

Sample	Shell	C. N.	R(Å)	σ^2 (Å^2)	ΔE_0 (eV)	R factor
$Pt_1Pd(111)/TiO_2$	Pt–Pd	3.4±5.3	2.4±0.07	0.013±0.025	-2.5±4.6	0.021
	Pt–Pd–Pt	8.6±4.6	2.7±0.04	0.042±0.062		
$Pt_1Pd(100)/TiO_2$	Pt–Pd	2.6±2.8	2.4±0.03	0.004±0.013	7.2±2.1	0.019
	Pt–Pd–Pt	10.8±3.7	2.7±0.02	0.024±0.042		